Pamukkale Univ Muh Bilim Derg, 26(3), 496-504, 2020

Pamukkale Üniversitesi Mühendislik Bilimleri Dergisi

Pamukkale University Journal of Engineering Sciences

Remediation of Cr(VI)using $C_3N_4/DEU-51(Fe)$under sun light irradiation

Güneş ışığı altında $C_3N_4/DEU-51(Fe)$ kullanılarak Cr(VI)'nın giderimi

Sevil AKÇAĞLAR[1*]

[1]Mechanical Engineering, Engineering Faculty, Dokuz Eylül University, Izmir, Turkey.
sevil.akcaglar@deu.edu.tr

Received/Geliş Tarihi: 29.01.2019, Revision/Düzeltme Tarihi: 12.04.2019 doi: 10.5505/pajes.2019.38468
Accepted/Kabul Tarihi: 26.04.2019 Research Article/Araştırma Makalesi

Abstract

A hybrid nanocomposite namely $C_3N_4/DEU-51(Fe)$ was developed to reduce the $Cr(VI)$ from a textile industry wastewater. $C_3N_4/DEU-51(Fe)$ exhibited a good cristalinity. The photocatalytic reaction of the carboxyl groups of the composite is in center and it is associated with the C-H-vibration. The optimal doping content of $C_3N_4/DEU-51(Fe)$ was determined to be 1.2 mg/L to treat 1.6 mg/L $Cr(VI)$ with a maximum yield of 98% at a sun light power of 80 mW/m² after 15 min at 42 °C in summer. After 5th times sun light experiments, the $C_3N_4/DEU-51(Fe)$ was reused with a yield of 97%. The $Cr(VI)$ reduction was explained with the Langmuir-Hinshelwood (L-H) kinetic model.

Keywords: Cr(VI), C_3N_4/DEU − 51(Fe), Langmuir-Hinshelwood photo-degradation kinetic, Reuse, Sun light.

Öz

$C_3N_4/DEU-51(Fe)$ hibrit nanokompoziti bir tekstil endüstrisi atık suyundaki $Cr(VI)$'yı azaltmak için geliştirilmiştir. $C_3N_4/DEU-51(Fe)$ kristal özellikli olup bu kompozitin merkezindeki karboksil gruplarının fotoparçalanma reaksiyonu C-H bağlanmasıyla ilgilidir. 1.6 mg/L $Cr(VI)$'yı yaz ayında %98'lik maksimum verimle gidermek için optimum koşullar; 1.2 mg/L $C_3N_4/DEU-51(Fe)$, 15 dk. temas süresi, 80 mW/m² güneş ışığı şiddeti ve 42 °C sıcaklıktır. $C_3N_4/DEU-51(Fe)$nanopartikülü 5 kez kullanıldıktan sonra %97 verimle geri kullanılmıştır. $Cr(VI)$ giderimi Langmuir-Hinshelwood (L-H) kinetik modelle açıklanmıştır. $Cr(VI)$ giderimi Langmuir-Hinshelwood (L-H) kinetik modelle açıklanmıştır.

Anahtar kelimeler: Cr(VI), C_3N_4/DEU − 51(Fe), Langmuir-Hinshelwood foto parçalanma kinetiği, Geri kullanım, Güneş Işığı.

1 Introduction

Heavy metal pollution is increasing significantly since the disposal of wastewater is an important environmental problem. Wastewaters from chemical, textile, glass and metal industries includes toxic heavy metals at high concentrations [1]-[3]. The environmental pollution caused by organic and inorganic pollutants increase the pollution problem because of rapid industrialization. Metals released to aquatic ecosystems as a result human activities, from soils and rocks concerning the discharge of metals from metal, chemical, petrochemical and metallurgical industries [4]. The big part of heavy metal pollutants are zinc, chromium, nickel and lead [5]. (Cr(VI)) is a metal present in the receiving aquatic ecocystems released wastewaters like metal, petrochemical, textile, leather and metal finishing [6]-[9].

The utilization of photo catalysts under sunlights increase the photodegradation mechanism by elevating the removal of resistant compounds. With good absorption under cross-section areas under solar spectrum, increase the conversion efficiency of pollutant in different environments with low cost [7],[10]. Cost is very significant in the comparison of the efficiency of the nano-adsorbents. A nono adsorbent should be cost effective. Improved adsorption capacities should be attributed to the low cost of adsorbents [11],[12]. With photocatalytic applications metals oxides can be converted to the other metals under UV light. The adsorbents it is used successfully in the removals of expensive by the industries and cause to environmental pollution [13]. Therefore, it is important to generate some cheap new metal-free catalysts activated under sun light and exhibiting good photocatalytic performance and they are friendly in environmental ecosystems [14]. For this reason, degradation of Cr(VI) to Cr(III) can be usefull for the environment and ecosystem.

In this study, Fe-based carbon nitride C_3H_4 nanocomposite was developed under laboratory conditions and it was used to reduce Cr(VI). The different concentrations of C_3N_4 (0.05 mg/L, 0.1, 0.3, 0.7, 1.0, 1.5, 2.3 and 5 mg/L) in C_3N_4/DEU − 51(Fe), the effects of increasing photooxidation times (5 min, 15 min, 35 min, 60 min and 90 min), the effects of increasing sun light powers (25 mW/m² at 12:00 in winter, 80 mW/m² at 12:00 in summer, 55 mW/m² at 12:00 in spring and 35 mW/m² at 12:00 in autumn), effect of temperature (10 °C in winter at 12:00; 23 °C in spring, at 12:00; 42 °C in summer at 12:00 and 26 °C in autumn at 12:00), effect of pH (2, 7 and 10) on the removals of Cr(VI) were researched. The reusability performance of C_3N_4/DEU − 51(Fe) and the Cr(VI) reduction by Langmuir-Hinshelwood kinetic model was researched.

2 Materials and methods

2.1 Production of DEU-51(Fe) under laboratory conditions

1,4-benzenedicarboxylate (1.4-BDC) (1.69 g) and $FeCl_36H_2O$ (2.12 g) were added into 50 mL N, N-dimethylformamide (DMF) and was mixed in a magnetic stirrer homogeneously. Then they were transferred into a 100 mL Teflon cap and it was incubated at 150 °C for 24 h. It was cooled in room temperature. The product was centrifugated, then it was rinsed with DMF and ethanol, respectively. The obtained sample dehydreted in an incubator at 150 °C for 24 h [15].

*Corresponding author/Yazışılan Yazar

2.2 Production of C_3N_4 under laboratory conditions

The C_3N_4 was produced with calcination of melamine [16]. 1.3 g melamine was added into a ceramic cup containing a cover, and then the produced matter was boiled at 560 °C in an incubator for 6 h. The product was utilized to produce the composite [15].

2.3 Production of $C_3N_4/DEU-51(Fe)$ under laboratory conditions

3 g C_3N_4 was put into10 mL DMF. This mixture ultrasonicated for 35 min. 1.76 g of 1.4-BDC and 4.89 g $FeCl_36H_2O$ were transferred to 56 mL DMF. They stirred until became homogenous. C_3N_4/DMF was successively settled in the mixture. It heated at an furnace of 150 °C for 1 day. The products were CMFe-3 and CMFe-5. They identified based on C and N (3 % and 5 %) percentages [15].

2.4 Photocatalytic removal of Cr(VI)

The photodegradation yield was measured by removing of Cr(VI) to Cr(III). Using different $C_3N_4/DEU-51(Fe)$ (0.1 mg/L, 0.3, 0.8, 1, 1.2, 1.6, 1.8, 2.5 and 4 mg/L) concentrations the reducing of 6 mg/L initial Cr(VI) solution were investigated.

2.5 Solar reactor

The solar reactor was made from a resistant quartz material with a volume of 1.9 L (30 cm heigth and 4 cm diameter). The UV studies were performed under constant sun ligths at powers varying between 70.00-80.00 mW/m² at hours between 11:00 am and 16:00 pm when the sunligth powers were at maximum levels.

2.6 Power of sunlight

The intensities of sunlight photoreactor were 25 mW/m² at 12:00 in winter, 80 mW/m² at 12:00 in summer, 55 mW/m² at 12:00 in spring and 35 mW/m² at 12:00 in autumn. Sunlight powers were measured with a Philips light meter Model DL-2001 during months and days.

2.7 Measurements of Cr(VI) and Cr(III) concentrations

Cr(VI) was detected in an chromatographic device containing a visible wavelength detector. The IC/PCR distinguish the Cr^{+6} as $CrO^4 =$ from other diphenyl reactions with carbazide. Reduction Cr(III) to Cr(VI) was performed according to the literature given by Gürkan et al. [17]. The pH was regulated to pH 10 by adding 15 mL 4% (w/w) H_2O_2. This sol was heated in an incubator at 80 °C during 50 min. Then it was boiled in a heater for 15 min to treat the H_2O_2. Cr(VI) was calculated in a spectrophotometer at a wave length of 651 nm. Cr(III) was measured by discarding Cr(VI) level from the total Cr.

2.8 Characterization of C_3N_4, DEU-51(Fe) and $C_3N_4/DEU-51(Fe)$

X-Ray Diffractometer (XRD) running at 40 mA and 40 kV (Cu-K) was used while a Fourier Transform Infrared (FTIR) spectroscopy on KBr was utilized in a Transmission FTIR Spectrometric Analyzer. Transmission Electron Microscope (TEM) and Scanning Electron Microscope (SEM) data were collected by using TEM JEM-200 CX with an electrical voltage of 100 kV. Brunauer, Emmet and Teller (BET) analysis were performed to determine the surrounding area, the pore volume and the pore size distribution of the adsorbent using nitrogen adsorption method.

3 Results and discussion

3.1 XRD patterns of C_3N_4, DEU-51(Fe) and $C_3N_4/DEU-51(Fe)$ for 0.5 mg, 1.0 and 2.0 mg

The crystal composition of DEU-51(Fe) was researched using XRD. The XRD pathways of DEU-51(Fe) exhibiting similar data with the study's results by Akple et al. and Wen et al. $C_3N_4/DEU-51(Fe)$, C_3N_4 and DEU-51(Fe) [18],[19] (Figure 1a). The strong diffraction hills of DEU-51(Fe) showing the crystalloid structure of this adsorbent. The raised peaks in XRD pathways exhibited similarities with the studies performed recently [20]. The small hills results from the breathing of some small molecular organics in the solvents used in the production of DEU-51(Fe) (Figure 1a). Some solvents, like DMF and BDC leads to production of important changes of the lattice in the hill peaks. The distinctions peaks of C_3N_4 exhibited similar data with the results of Lewellyn et al. and Hu et al. (Figure 1b) [21],[22]. The interlayer-stacking hill (0019) at 29.8 °C attributed to the interlayer distance of ~0.38 nm in the structure of C_3N_4. The XRD patterns of $C_3N_4/DEU-51(Fe)$ showed a crystal constitution of the DEU-51(Fe). It was not varied after the supplementation of C_3N_4 as reported by Wang et al. and Hong et al. [23],[24]. Figure 1c, indicates the XRD-patterns of 0.5 mg, 1.0 and 2.0 mg $C_3N_4/DEU-51(Fe)$. It was shown that the XRD pathways of the this composite exhibited similarities with the XRD patterns of DEU-51(Fe) and C_3N_4. This showed that the crystal constitution of the DEU-51(Fe) is not varied after the supplementation of C_3N_4. This result agree with the previous recent investigations [24],[25].

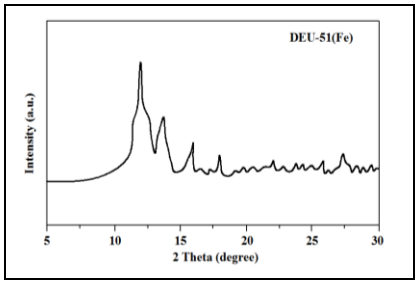

Figure 1a. XRD patterns of DEU-51(Fe).

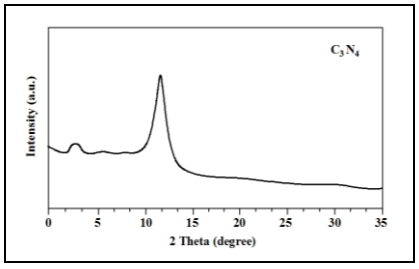

Figure 1b. XRD patterns of C_3N_4.

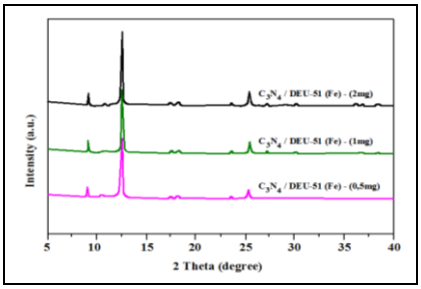

Figure 1c. XRD patterns of $C_3N_4/DEU-51(Fe)$.

3.2 FTIR spectra of C_3N_4, DEU-51 (Fe) and $C_3N_4/DEU-51(Fe)$

The spectra of C_3N_4 and the other constituents of nanocomposites are illustrated in Figure 2. This spectrum involved broad exceed bands at 3271 cm^{-1}, 3164 cm^{-1}, and 3072 cm^{-1}. These bands are related with the stretching pulses of N-H bonds. More specific bands were detected at 1636 cm^{-1}, 1569 cm^{-1}, 1410 cm^{-1}, 1326 cm^{-1}, 1242 cm^{-1} and 806 cm^{-1} indicating the characteristic of C_3N_4 [21],[22],[24]. Powerful bands around 1636 cm^{-1} and 1242 cm^{-1} such as C=N and C-N illustrated different cyclic rings. The FTIR spectra of DEU-51(Fe) showed in Figure 2. This graph showed similar data based on vibration their structure. This contains trivalent metal cores and -COOH ligands. The absorption apicals of the DEU-51(Fe) were detected at around 1685 cm^{-1}, 1595, 1396, 1020, and 750 cm^{-1}. These hills were originated from the oscillation in the COOH groups compared to the recent literatures [26],[27]. The high intensity of (C-O) at around 1685 cm^{-1} indicates the availability of some free carboxylic groups [28]. The two strong peaks at around 1595 and 1396 cm^{-1} ((C-O) and (C-O)) exhibited the derivatives of carboxyl groups. This indicates the availability of Fe containing nanocomposites for effective adsorption. The FTIR spectrum of $C_3N_4/DEU-51(Fe)$-(0,5 mg; 1 and 2 mg) exhibits two bands at 1564 cm^{-1} and 1383 cm^{-1} (Figure 2). This is related with the absorption of the carboxyl groups on the center of $C_3N_4/DEU-51(Fe)$ composite. The strong band at 747 cm^{-1} is relevant to C-H-puls. Both samples showed the same frequency dependence in the construction of nanocomposite. This showed that the structure of $C_3N_4/DEU-51(Fe)$ composite was not changed effectively.

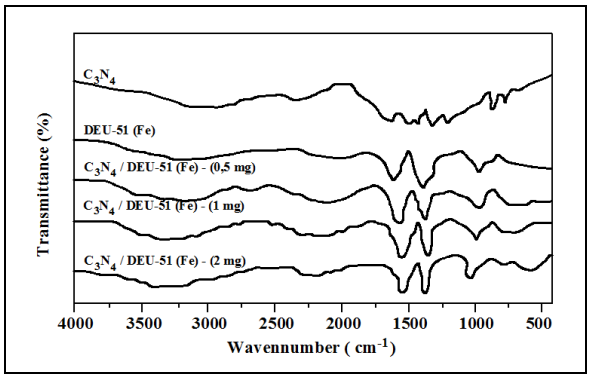

Figure 2. FTIR spectra of C_3N_4, DEU-51(Fe) and $C_3N_4/DEU-51(Fe)$.

3.3 SEM images of DEU-51(Fe), $C_3N_4/DEU-51(Fe)$; and TEM micrographs of C_3N_4, DEU-51(Fe)

As shown in Figure 3a, SEM images of DEU-51(Fe) exhibited a multiple hedron structure. The SEM picture of $C_3N_4/DEU-51(Fe)$ composite reveals C_3N_4 coated on the DEU-51(Fe) showed similarities with the surface of composite (Figure 3b). Figure 3c exhibited the TEM micrographs of C_3N_4 and DEU-51(Fe). This showed that the C_3N_4 was greatly localized to the superficies of the $C_3N_4/DEU-51(Fe)$ composite.

3.4 EDS measurement of C_3N_4/DEU-51(Fe)

EDS analysis results showed that there are iron, carbon, oxygen and nitrogen elements in the structure of $C_3N_4/DEU-51(Fe)$ composite (Figure 4). The elements were distributed throughout $C_3N_4/DEU-51(Fe)$ composite.

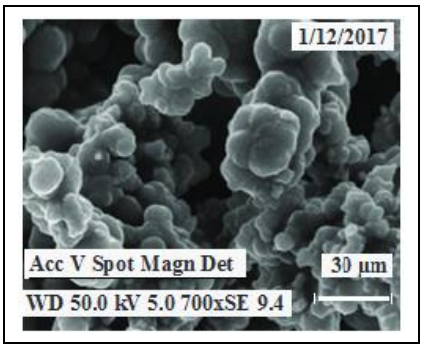

Figure 3(a). DEU-51(Fe).

Figure 3(b). $C_3N_4/DEU-51(Fe)$.

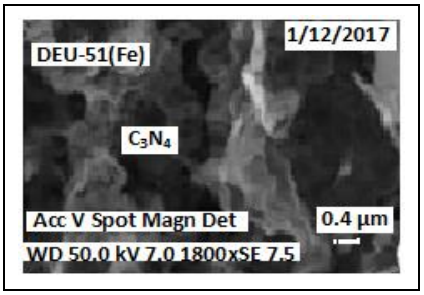

Figure 3(c). C_3N_4 and DEU-51(Fe).

Figure 3. SEM images of DEU-51(Fe) (a) and $C_3N_4/DEU-51(Fe)$(b); TEM images of C_3N_4 and DEU-51(Fe)(c).

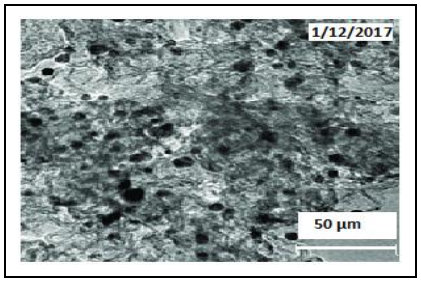

Figure 4. EDS measurement composite.

3.5 BET, pore volume and pore diameter analysis of C_3N_4, DEU-51(Fe) and $C_3N_4/DEU-51(Fe)$

The BET surface area of $C_3N_4/DEU-51(Fe)$ complete composite is 22.04 $m^2\ g^{-1}$. It is over than pristine C_3N_4 (13.5 $m^2\ g^{-1}$) and DEU-51(Fe) (12.8 $m^2\ g^{-1}$) (Table 1). The mean pore radius of $C_3N_4/DEU-51(Fe)$ composite containing Cr(VI) is also bigger than that of pristine $C_3N_4/DEU-51(Fe)$ composite before Cr(VI) treatment. This can be explained with the surface of composite which is not occupied by C_3N_4.

The introduction of the C_3N_4 to the $C_3N_4/DEU-51(Fe)$ composite does not influence the generation of the pure composite crystals to a certain extend.

3.6 Effects of doping content of C_3N_4 in the 1.6 mg/L $C_3N_4/DEU-51(Fe)$ on the treatment of initial 6 mg/L Cr(VI) at a sun light power of 65 mW/m² after 14 min photoxidation

The effect of C_3N_4 dose on the photocatalytic treatment of Cr(VI) was investigated for limits varying between 0.05-5.0 mg/L. The efficiencies were compared with a sample without catalyst. This phenomenon was determined as photolysis. Furthermore, a control was utilized to research the adsorption and desorption of Cr(VI) on the C_3N_4 surface under sun light. As the C_3N_4 concentration was increased from 0.05 mg/L up to 0.7 mg/L, the Cr(VI) concentrations reduced to 0.83 mg/L with a Cr(VI) yield of 93 % (Table 2). Further increase of C_3N_4 concentration up to 2.3 and 5.6 mg/L the Cr(VI) removals remained stable. The maximum Cr(VI) yields was obtained at 0.70 mg/L C_3N_4 concentration. About 0,8-1,2 % removal in the level of Cr(VI) was detected after 20 min of adsorption under dark circumtances. The level of Cr (VI) did not modify during 60 min (data not shown). For this reason, the Cr (VI) mixed with the C_3N_4 during 10 min in order to reach the steady-state conditions for adsorption and desorption processes under dark conditions. It was not found a big removal in the Cr (VI) concentrations during photolysis. However addition of 0,7 mg/L of C_3N_4 catalyst increase the photodegradation of pollutant. At a lower C_3N_4 concentrations (0.05 and 0.1 mg/L) the Cr(VI) removal yield was 45-55 % after 15 min photocatalysis. When the C_3N_4 level increased (0.30 mg/L and 0.7 mg/L); 65% and 93% Cr (VI) treatment efficiencies was observed, respectively. The increasing of the C_3N_4 catalyst (1.00 mg/L, 1.50 and 5 mg/L) lowered the yield of Cr (VI) (92%). Therefore, 0.7 mg/L C_3N_4 was accepted as an optimum concentration for the studies performed during the experiments. At his C_3N_4 levels the photocatalytic yield for Cr(VI) removal was detected via good electron transferring during effective sun light absorption. The optimum catalyst concentration was chosen when the reactive oxygen species are optimum to remove the Cr (VI). Optimum concentration can be defined as the equilibrium between free radicals and shifting due to the presence of excess C_3N_4. Similarly, Huang at al. also detected an optimum g-C_3N_4 concentration in the g-C_3N_4, MIL-53(Fe) showed better Cr(VI) yield, compared to MIL-53(Fe) [15]. It was declared that high electron migration yield exhibits an important way to rise the photocatalytic yield. This is very important since rich electron transfer can decrease the redox of electron-cavity pairs [15]. Wan et al. and Wang et al. investigated the impact of nanocomposite level on photodegradaion of Cr(VI) under visible light. They observed efficient Cr(VI) yield (85%) under sunlight using 0.8 g/L g-C_3N_4/graphene under optimum conditions [29],[30].

3.7 Effects of $C_3N_4/DEU-51(Fe)$ concentrations on the treatment of Cr(VI) at 0,7 mg/L C_3N_4 concentration at initial 6 mg/L Cr(VI) at a sun light power of 65 mW/m² after 14 min photooxidation

$C_3N_4/DEU-51(Fe)$ levels were raised from 0.1 mg/L up to 4 mg/L. As the $C_3N_4/DEU-51(Fe)$ level was enhanced from 0.1 mg/L up to 1.2 mg/L the Cr(VI) yields increased from 34% up to 93% (Table 3). Further increase of this nanocomposite did not affect the Cr(VI) removals. The effective Cr(VI) photooxidation was obtained at 1.2 mg/L $C_3N_4/DEU-51(Fe)$ levels. The lowest Cr(VI) photooxidation was obtained at 0.1 mg/L $C_3N_4/DEU-51(Fe)$ levels as 34%. An increase of $C_3N_4/DEU-51(Fe)$ loading advices to elevate the activated regions, however, can be decrease the reduction of Cr(IV) by blocking sun irradiation.

Nguyen and Juang reported that the increase of catalyst increased the reduction efficiency of pollutant because catalyst exhibits a high capacity for promoting the intreaction between oh radicals and pollutants [31]. In this study, $C_3N_4/DEU-51(Fe)$ $C_3N_4/DEU-51(Fe)$ exhibited a high Cr(VI) reduction, however when the $C_3N_4/DEU-51(Fe)$ concentration increased from 1. 6 mg/L up to 4.0 mg/L, no significant improvement of Cr(VI) decrease was observed. When the catalyst concentration is higher than that an optimal value [$C_3N_4/DEU-51(Fe)$ catalyts concentration (>1.2 mg/L)]; excess photocatalyst would cause accumulation of nano composite which is independent and elevated the opacity.

Table 1. Surface Properties of $C_3N_4/DEU-51(Fe)$.

Samples	BET(m^2g^{-1})[a]	V(ccg^{-1})[b]	D(nm)[c]
$C_3N_4/DEU-51(Fe)$ (1.6 mg)	22.04	0.093	1.92
C_3N_4 (0.70 mg)	13.50	0.021	1.42
$C_3N_4/DEU-51(Fe)$ (0.5 mg)	17.90	0,067	1.72
$C_3N_4/DEU-51(Fe)$ 1 mg)	18.50	0,076	1.83
$C_3N_4/DEU-51(Fe)$ (2 mg)	19.90	0.081	1.79
DEU-51(Fe) (0.90 mg)	12.80	0.070	1.45

[a]: BET specific surface. [b]: Total pore volüme. [c]: The pore diameter.

Table 2. Effects of doping content of C_3N_4 in the 1.6 mg/L $C_3N_4/DEU-51(Fe)$ on the removals of Cr(VI).

C_3N_4 Concentration (mg/L)	Cr(VI) Concentration (mg/L)	Cr(VI) removal efficiency (%)	Cr(III) Concentration (mg/L)after Photocatalysis	Remaining Cr(VI) Concentration (mg/L)
0.05	6	45	1.60	3.30
0.10	6	55	1.80	2.70
0.30	6	65	2.20	2.10
0.70	6	93	5.59	0.42
1.00	6	92	5.52	0.48
1.50	6	92	5.52	0.48
2.30	6	92	5.52	0.48
5.00	6	92	5.52	0.48

Table 3. Effects of $C_3N_4/DEU-51(Fe)$ concentrations on the removal of Cr(VI).

$C_3N_4/DEU-51(Fe)$ Concentration (mg/L)	Cr(VI) concentration (mg/L)	Cr(VI) removal efficiency (%)	Cr(III) concentration (mg/L) after photocatalysis	Remaining Cr(VI) concentration (mg/L)
0.1	6	34	1.10	3.96
0.3	6	55	1.40	2.70
0.8	6	65	1.70	2.10
1.0	6	70	2.20	1.80
1.2	6	93	5.58	0.42
1.6	6	91	5.52	0.54
1.8	6	91	5.52	0.54
2.5	6	91	5.52	0.54
4.0	6	91	5.52	0.54

However, this cause a reduction in sun ligth distibution in order to protect the effect of some solid particles [32]. At high nanocomposite levels in aquatic media asteric effect can be observed. Under these conditions the granule-granule interaction can musk the sun ligth diffusation and lowered the active reaction sites.

3.8 Effect of photooxidation times under sun light at 1.2 mg/L $C_3N_4/DEU-51(Fe)$ concentrations on the removal of Cr(VI) at 0.7 mg/L C_3N_4 concentration at initial 6 mg/L Cr(VI) at a sun light power of 65 mW/m² after increasing photodegradation times (5 min, 15, 35, 60 and 90 min)

As the photooxidation times were increased from 5 min up to 15 min the Cr(VI) yields increased from 45% up to 93% under sun light (Table 4). The maximum Cr(VI) reduction to Cr(III) was found after 15 min contacting with 65 mW/m² sun light. Further increase of time did not affect the Cr(VI) removals. Data obtained from this study showed that the Cr(VI) reduction to Cr(III) depletes with attenuation of photodegradation period. It can speculated that longer retention time, in an elevated ratio of contact and at long contact times; hydroxyl radicals were not achieved for Cr(VI) reduction. As a result, low conversion rates was observed [33]. At a shorter residence time, Cr(III) have a lower colloid forming capacity with the OH anions produced from the photooxidation of Cr(VI) [33]. The enhancement effect is reduced with decreasing residence time. Jing et al. observed that the photoremoval efficiency of MIL-68(Fe) on the treatment of Cr(VI) in different media under UV light depends on illumination time [34]. The optimum illumination time for maximum removal of Cr(VI) (87%) was obtained as 60 min. In our study, the optimum time and the maximum Cr (VI) yields were found to be higher than the study by Jing et al. [34].

3.9 Effects of increasing sun light powers on the removals of Cr(VI) photoremovals at 1.2 mg/L $C_3N_4/DEU-51(Fe)$ concentration at 0.7 mg/L C_3N_4 concentration at initial 6 mg/L Cr(VI) at a sun light power of 65 mW/m² after 15 min photooxidation

As the sun light powers were increased from 25 mW/m² at 12:00 in winter to 80 mW/m² at 12:00 in summer; the Cr(VI) removals increased from 34 % up to 97% (Table 5). The Cr(VI) yields increased from 34% to 45%, to 78% and to 97% as the sun light powers increased during season. The Cr(VI) removals were at medium levels (45% and 78%) at medium sun light powers (35 and 55 mW/m²); since the sun was not so effective in the photooxidation. Sun light corresponds for the wavelength and gap energy of $C_3N_4/DEU-51(Fe)$ during contacting sun wavelength. The photon flux is important in the photocatalytic processes. The UV has a major influence in the removal of Cr(VI) since its influence in the production of OH • radicals at elevated amount. A rise in light strength cause to improve the photocatalytic rates. In this study contrarily to the studies performed by Asadi et al. at high sun light powers (55 and 80 mW/m² in spring and in summer) electron hole pairs did not separate and they did not compete with electron-hole recombination [35]. Zou et al. also mentioned that treatment of Cr(VI) and total chromium by Fe-nanoparticles depend on sun light powers [36]. They found that the majority of Cr(VI) presented in wastewater was likely reduced to Cr(III) at high sun light powers such as 80-90 mW/m².

3.10 Effect of pH on the Cr(VI) reductions

The studies were performed in the pH range (2,5-8,5) for 6 mg/L Cr(VI) dose and 1.2 mg/L of $C_3N_4/DEU-51(Fe)$ dosage and a C_3N_4 level of 0.7 mg/L at a temperature of 42 °C. Cr(VI) yield is relevant with pH and the maximum Cr(VI) yield (99.8%) is obtained at pH 2.5 (Table 6). The pH in the beginning of the study has an important effect on the Cr(VI) in wastewater, and this affect the photoremoval of Cr(VI) [37]-[41].

At high pH levels the removals of Cr(VI) depleted since pH pzc of $C_3N_4/DEU-51(Fe)$ is around 4.2 [41]. At negative surface charges the production of Cr(VI) species decreased. $HCrO_4^-$ accumulates under pH 4 and 5 and is sorbed on the nanocomposite superficial surface. At pH>3, important quantity of $Cr_2O_4^{2-}$ and $Cr_2O_7^{2-}$ were found [42],[43]. Cr(VI) yields raised at low pH values [44]. At pH 2.5, 99.8 % of the Cr(VI) decreased after 15 min. At pH of 5.0, and 8.5, the yield after 15 min irradiation were 60%, and 30%, respectively (Table 7). Cr(VI) reduction rates were maximum at acidic pH than at neutral or basic pH conditions. This can be explained by the big removal ratio of Cr(VI)/Cr(III) at lower pH.

As the pH was decreased, the main thermodynamic power for Cr(VI) removal increases [45]. At high pH, the molecular oxygen levels is higher than for the Cr(VI) and O_2. This resultnng in with low Cr(VI) yields. The Cr(VI) yield elevated at low pH, and improve the rate by corrosion of Fe. pH is one of the important since has an significant effect on photocatalysis [46]. At lower value of pH (5.0), the Cr(VI) yield was 60%. When the pH was 8.5, 30% removal was obtained. The results indicated that low pH was favorable for the removal of chromium. Under acidic pH condition, the electrostatic attraction between $C_3N_4/DEU-51(Fe)$ the and Cr ion increases. Jing et al., also observed that the low Cr(VI) yields via photodegradation was strongly effected by the pH value of the medium[34]. The Cr (VI) photooxidation percentage increased to 98 % when the pH increased to 3.0 [34],[47].

Table 4. Effects of photooxidation times on Cr(VI) removals at a sun light power of 65 mW/m².

$C_3N_4/DEU-51(Fe)$ Concentration (mg/L)	Photo oxidation time (min)	Cr(VI) concentration (mg/L)	Cr(VI) removal efficiency (%)	Cr(III) concentration (mg/L) after photocatalysis	Remaining Cr(VI) concentration (mg/L)
1.2	5.0	6	45	1.9	3.30
1.2	15	6	93	5.58	0.42
1.2	35	6	93	5.58	0.42
1.2	60	6	93	5.58	0.42
1.2	90	6	93	5.58	0.42

Table 5. Effects of sun light powers on Cr(VI) removals.

$C_3N_4/DEU-51(Fe)$ Concentration (mg/L)	Photooxidation power (mW/m²)	Photo oxidation time (min)	Cr(VI) Concentration (mg/L)	Cr(VI) removal efficency (%)	Cr(III) Concentration (mg/L) after photocatalysis	Remaining Cr(VI) Concentration (mg/L)
1.2	25 W/m² in winter	15	6	34	2.02	3.96
1.2	80W/m² In Summer	15	6	90	4.10	0.60
1.2	55 W/m² in spring	15	6	78	3.45	1.32
1.2	35 W/m² in autumn	15	6	45	2.45	3.30

Table 6. Effects of pH on Cr(VI) removals.

$C_3N_4/DEU-51(Fe)$ concentration (mg/L)	pH	Cr(VI) concentration (mg/L)	Cr(VI) removal efficiency (%)	Cr(III) concentration (mg/L) after photocatalysis	Remaining Cr(VI) concentration (mg/L)
1.2	2.5	6	99.8	5.70	0.012
1.2	5.0	6	60.0	2.40	2.400
1.2	8.5	6	30.0	1.02	4.200

Table 7. Langmuir Hinshelwood kinetic for photocatalytic reduction of Cr(VI).

$C_3N_4/DEU-51(Fe)$ Concentration (mg/L)	k_r (unitless)	K_{LH} (mg/L-min)	R^2
0.1	0.204	0.018	0.99
0.3	0.308	0.032	0.99
0.8	0.442	0.042	0.99
1.0	0.490	0.065	0.99
1.2	0.940	0.078	0.99
1.6	0.720	0.043	0.99

3.11 Photocatalytic removal mechanism of Cr(IV) by $C_3N_4/DEU-51(Fe)$

During photocatalysis $C_3N_4/DEU-51(Fe)$ is excited by sorption of electrons of sun light equivalent or bigger than the band gap Eg. This cause to exciting of a photon from the valence band to the conduction band. Eg of $C_3N_4/DEU-51(Fe)$ is around 2.4 eV, relevant to ca. 320 nm. For this reason, $C_3N_4/DEU-51(Fe)$ has to be affected with sun light. The photon-hollow redox reactions is a quick phenomenon (<80 split-second in a $C_3N_4/DEU-51(Fe)$ [48],[49]). With chemical processes the photon conduction proceses occurred between $h^+\nu_B$ or e^-_{CB} and different matters on the around of $C_3N_4/DEU-51(Fe)$ [50], [51]. The photon receivers decreased by photons in conduction band and releasing matters can be oxidized by $h^+\nu_B$ [52]. The redox reactions occurred between conduction band and valance band. Hydroxyl radicals ($HO\bullet$) releasing by the redox reaction between valence band and conduction band adsorbed to the wastewater and to the surrounding of the hydroxyls are oxidizing compounds [51]. The reactive oxygen species such as ($HO_2\bullet/O_2\bullet^-$), are also generated from Cr(III) by transformation of Cr(IV). Cr(V) and Cr(IV) can be dissolved and it can be reacted with Cr(V) and Cr(IV). Cr(III) can be oxidized by valence band/hydroxyl radical couple [37],[53],[55]. Cr(III) was obtained as the end product on the $C_3N_4/DEU-51(Fe)$ surface [53],[54],[56]. This is possible because the accumulation of Cr(III) cause to decrease the activation of $C_3N_4/DEU-51(Fe)$ and this prevents the transportation of the electrons by redox reactions [57],[58].

This provides very advantageous in the photocatalytic systems for Cr(VI) depletion from effluents. The mechanism responsible for the convertion of Cr(VI) to Cr(III) can be explained as follows: Cr(VI) in excited state could be reduced by the electron

donor in the conduction band of $C_3N_4/DEU-51(Fe)$ with the aid of H^+. The photoreduction of CrO_4 mediated by the electron donor in oxygenated textile industry wastewaters. The possible mechanism of the photochemical reduction of Cr(VI) was proposed following Eqs. 1-4 [57],[58].

$$Cr(VI) + ROH + OH^- + h\nu \rightarrow Cr(VI) + OH^- + H_2O \quad (1)$$

$$C_3H_4 / DEU-51(Fe) + h\nu \rightarrow h + [C_3H_4 / DEU-51(Fe^+)] + OH^- + e^-[C_3H_4 / DEU-51(Fe)] \quad (2)$$

$$e^-[C_3H_4 / DEU-51(Fe)] + OH^- \rightarrow e^-[C_3H_4 / DEU-51(Fe)] \quad (3)$$

$$Cr(VI) + OH^- + e^- \rightarrow Cr(III) + H_2O \quad (4)$$

3.12 Reusability of $C_3N_4/DEU-51(Fe)$

The photocatalytic activity of $C_3N_4/DEU-51(Fe)$ does not significantly reducted after sequential five cycles for the removal of Cr(VI) to Cr(III). This showed that $C_3N_4/DEU-51(Fe)$ exhibited high resistance and can be utilized for sequential removal of Cr(VI) photoreduction (Table 8).

Table 8. Recovery of $C_3N_4/DEU-51(Fe)$.

C_3N_4/ DEU – 51(Fe) (mg/L)	Cr(VI) removal (%) first	Cr(VI) removal (%) second	Cr(VI) removal (%) third	Cr(VI) removal (%) fourth	Cr(VI) removal (%) five
1,2 RUN -1	98	98	98	97	97
1,2 RUN -2	98	98	98	97	97
1,2 RUN -3	98	98	97	97	96

4 Conclusions

$C_3N_4/DEU-51(Fe)$ was produced in a research laboratory and can be used was as a heterocatalyst to remove Cr(VI) from wastewater under sun-light applications. The novel composite is effective of Cr(VI) removal. pH has a successfully effect on the removal of Cr(VI) photodegradation under a sun light power of 80 mW/m². XRD analysis showed that $C_3N_4/DEU-51(Fe)$ exhibited good crystallinity. The FTIR spectrums showed that the corresponded bands in the photocatalytic reaction are related to carboxyl groups of the composite center and it is associated with the C-H-vibration. The TEM micrographs showed that C_3N_4 was present in the $C_3N_4/DEU-51(Fe)$. The optimum pH in Cr(VI) removal by $C_3N_4/DEU-51(Fe)$ was found at pH 2,5. Cr(VI) was reduced with a maximum yield of 92% to Cr(III) at 0.7 mg/L C_3N_4 concentration using 1.2 mg/L $C_3N_4/DEU-51(Fe)$ composite concentration after 15 min photooxidation time in summer at 42 °C. The photocatalytic performance of $C_3N_4/DEU-51(Fe)$ was enhanced by doping of C_3N_4. The photo-catalytic reduction rate of Cr(VI) was expressed by Langmuir-Hinshelwood Kinetic Model. The k_r and the K_{LH} were obtained as 0.940 unitless and 0.078 mg/L-min, respectively. $C_3N_4/DEU-51(Fe)$ was reused with a Cr(VI) yield of 97% after five sequential treatment trips.

5 References

[1] Zhao G, Li J, Ren X, Chen C, Wang X. "Few-layered graphene oxide nano sheets as superior sorbents for heavy metal ion pollution management". *Environmantal Science and Technology*, 45, 10454-10462, 2011.

[2] Ross D, Ketterings Q. *Recommended Methods for Determining Soil Cation Exchange Capacity*. Publisher University of Delaware Newark DE, Northeastern United States, 1995.

[3] Mohammed AS, Kapri A, Goel R. "Heavy metal pollution: source, impact and remedies". *Biomanagement of Metal-Contaminated Soils,* 9(1), 1-28, 2011.

[4] Aremu MO, Atolaiye BO, Labaran L. "Environmental implication of metal concentrations in soil, plant foods and pond in area around the derelict udege mines of nasarawa state". *Nigeria Chemical Society Ethiopia*, 24(3), 351-360, 2010.

[5] Kieber RJ, Willey JD, Zvalaren SD. "Chromium speciation in rainwater: temporal variability and atmospheric deposition". *Environmantal Science and Technology*, 36, 5321-5327, 2002.

[6] Testa JJ, Grela MA, Litter MI."Heterogeneous photocatalytic reduction of chromium (VI) over TiO_2 particles in the presence of oxalate: involvement of Cr(VI) species". *Environmental Science and Technology*, 38, 1589-1594, 2014.

[7] Qiu B, Xu CX, Sun DZ, Wei HG, Zhang X, Guo J, Wang Q, Rutman D, Guo ZH, Wei SY. "Polyaniline coating on carbon fiber fabrics for improved hexavalent chromium removal". *RSC Advances,* 4, 29855-29865, 2014.

[8] Lv ZF, Liang CS, Cui JY, Zhang YA, Xu S. "A facile route for the synthesis of mesoporous melamine-formaldehyde resins for hexavalent chromium removal". *RSC Advances*, 5, 18213-18217, 2015.

[9] Cai L, Xiong X, Liang N, Long Q. " Highly effective and stable Ag_3PO_4-WO_3/MWCNTs photocatalysts for simultaneous Cr(VI) reduction and orange II degradation under visible light irradiation". *Applied Surface Science*, 353, 939-948, 2015.

[10] Rajeshwar K, Chenthamarakshan CR, Goeringer S, Djukic M. "Titania-based heterogeneous photocatalysis. Materials, mechanistic issues, and implications for environmental remediation". *Pure and Applied Chemistry*, 73(12), 1849-1860, 2001.

[11] Bailey SE, Olin TJ, Bricka RM, Adrian DD. "A review of pontentially low-cost sorbents for heavy metals". *Water Research*, 33(11), 2469-2479, 1999.

[12] Dresselhaus MS, Thomas IL. "Alternative energy technologies". *Nature*, 414, 332-337, 2014.

[13] Maeda K, Takata T, Ha M, Saito N, Domen KJ. "GaN: ZnO solid solution as a photocatalyst for visible-light-driven overall water splitting". *American Chemical Society*, 127, 8286-8287, 2005.

[14] Niu S-f, Liu Y, Xu X-h, Lou Z-h. "Removal of hexavalent chromium from aqueous solution by iron nanopartlcles". *Journal of Zhejiang University*, 6B(10), 1022-1027, 2005.

[15] Huang W, Liua N, Zhanga X, Wub M, Tang L. "Metal organic framework g-C_3N_4/MIL-53(Fe) heterojunctions with enhanced photocatalytic activity for Cr(VI) reduction under visible light". *Applied Surface Science*, 425, 107-116, 2017.

[16] Niu P, Zhang L, Liu G, Cheng H-M. "Graphene-like carbon nitride nanosheets for improved photocatalytic activities". *Advanced Functional Materials*, 22, 4763-4770, 2012.

[17] Gürkan R, Ulusoy HI, Akçay M. "Simultaneous determination of dissolved inorganic chromium species in wastewater/natural waters by surfactant sensitized catalytic kinetic spectrophotometry". *Arabian Journal of Chemistry*, 10, 450-460, 2017.

[18] Akple MS, Low J, Wageh S, Al-Ghamdi AA, Yu J, Zhang J. "Enhanced visible light photocatalytic H_2-production of g-C_3N_4/WS2 composite heterostructures". *Applied Surface Science*, 358, 196-203, 2015.

[19] Wen J, Xie J, Yang Z, Shen R, Li H, Luo X, Li X. "Fabricating the robust g-C_3N_4 nanosheets/carbons/NiS multiple heterojunctions for enhanced photocatalytic H_2 generation: an insight into the trifunctional roles of nanocarbons". *ACS Sustain, Chemical Engineering*, 5(3), 2224-2236, 2017.

[20] Cao K, Jiang Z, Zhang X, Zhang Y, Zhao J, Xing R, Yang S, Gao C, Pan F. "Highlywater-Selective hybrid membrane by incorporating g-C_3N_4 nanosheets into polymer matrix". *Journal of Membrane Science*, 490, 72-83, 2015.

[21] Llewellyn PL, Horcajada P, Maurin G, Devic T, Rosenbach N, Bourrelly S, Serre C, Vincent D, Loera-Serna S. "Linear alkanes in the flexible metal-organic-framework MIL-53(Fe)". *Journal of the American Chemical Society*, 131, 13002-13008, 2009.

[22] Hu SZ, Ma L, You JG, Li FY, Fan ZP, Wang F, Liu FD, Gui JZ. "A simple andefficient method to prepare a phosphorus modified g-C_3N_4 visible light photocatalyst". *RSC Advances*, 4, 21657-21663, 2014.

[23] Wang H, Yuan XZ, Wu Y, Zeng GM, Chen XH, Leng LJ, Li H. "Synthesis and applications of novel graphitic carbon nitride/metal-organic frameworks mesoporous photocatalyst for dyes removal". *Applied Catalysis B*, 174, 445-454, 2015.

[24] Hong J, Chen C, Bedoya FE, Kelsall GH, O'Hare D, Petit C. "Carbon nitridenanosheet/metal-organic framework nanocomposites with synergistic photocatalytic activities". *Catalysis Science & Technology*, 6, 5042-5051, 2016.

[25] Du JJ, Yuan YP, Sun JX, Peng FM, Jiang X, Qiu LG, Xie AJ, Shen YH, Zhu JF. "New photocatalysts based on MIL-53 metal-organic frameworks for the decolorization of methylene blue dye". *Journal of Hazardous Materials*, 190, 945-951, 2011.

[26] He F, Chen G, Zhou Y, Yu Y, Zheng YS. "The facile synthesis of mesoporous g-C_3N_4 with highly enhanced photocatalytic H_2 evolution performance". *Chemical Communications*, 51(90), 16244-16246, 2015.

[27] Zhu Z, Murugananthan M, Gu J, Zhang Y. "Fabrication of a Z-scheme g-C_3N_4/Fe-TiO_2 photocatalytic composite with enhanced photocatalytic activity under visible light". *Irradiation Catalysts*, 8(3), 112-120, 2018.

[28] Zheng Y, Jiao Y, Chen J, Liu J, Liang J, Du A, Zhang W, Zhu Z, Smith SC, Jaroniec M, Lu GQ, Qiao SZ. "Nanoporous Graphitic-C_3N_4@Carbon Metal-free electrocatalysts for highly efficient oxygen reduction". *Journal of the American Chemical Society*, 133(50), 20116-20119, 2011.

[29] Wan SL, He F, Wu JY, Wan WB, Gu YW, Gao B, Hazard J. "Rapid and highly selective removal of lead from water using graphene oxide-hydrated manganese oxide nano composites". *Journal of Hazardous Materials*, 314, 32-40, 2016.

[30] Wang X, Liang Y, An W, Hu J, Zhu Y, Cui W. "Removal of chromium (VI) by a self-regenerating and metal free g-C_3N_4/graphene hydrogel system via the synergy of adsorption and photo-catalysis under visible light". *Applied Catalysis B: Environmental*, 219, 53-62, 2017.

[31] Nguyen AT, Juang RS. "Photocatalytic degradation of p-chlorophenol by hybrid H_2O_2 and TiO_2 in aqueous suspensions under UV irradiation". *Journal of Environmental Management*, 147, 271-277, 2015.

[32] Zeghioud H, Khellaf N, Djelal H, Amrane A, Bouhelassa M. "Photocatalytic reactors dedicated to the degradation of hazardous organic pollutants: kinetics, mechanistic aspects and design". *Chemical Engineering Communications*, 203, 1415-1431, 2016.

[33] Zuo Y, Zhan, J, Wu T. "Effects of Monochromatic UV-Visible Light and Sunlight on Fe(III)-Catalyzed Oxidation of Dissolved Sulfur Dioxide". *Journal of Atmospheric Chemistry*, 50, 195-210, 2005.

[34] Jing F, Liang R, Xiong J, Chen R, Zhang S, Li Y. "MIL-68 (Fe) as an efficient visible-light-driven photocatalyst for the treatment of a simulated waste-water contain Cr (VI) and Malachite Green". *Applied Catalysis B: Environmental*, 206, 9-15, 2017.

[35] Assadi AA, Palau J, Bouzaza A, Wolbert D. "Modeling of a continuous photocatalytic reactor for isovaleraldehyde oxidation: Effect of different operating parameters and chemical degradation pathway". *Chemical Engineering Research and Design*, 91(7), 1307-1316, 2013.

[36] Zou Y, Wang X, Khan A, Wang P, Liu Y, Alsaedi A, Hayat T, Wang X. "Environmental remediation and application of nanoscale zero-valent iron and its composites for the removal of heavy metal ions". *Environmental Science and Technology*, 50(14), 7290-7304, 2016.

[37] Testa JJ, Grela MA, Litter MI. "Experimental evidence in favor of an initial one-electron-transfer process in the heterogeneous photocatalytic reduction of chromium (VI) over TiO_2". *Langmuir*, 17, 3515-3517, 2001.

[38] Das DP, Parida K, De BR. "Photocatalytic reduction of hexavalent chromium in aqueous solution over titania pillared zirconium phosphate and titanium phosphate under solar radiation". *Journal of Molecular Catalysis A: Chemical*, 245, 217-224, 2006.

[39] Wang L, Wang N, Zhu L, Yu H, Tang H. "Photocatalytic reduction of Cr(VI) over different TiO_2 photocatalysts and the effects of dissolved organic species". *Journal of Hazardous Materials*, 152(1), 93-99, 2008.

[40] Guo D, Wen R, Liu M, Guo H, Chen J, Weng W. "Facile fabrication of g-C_3N_4/MIL-53(Al) composite with enhanced photocatalytic activities under visible-light irradiation". *Applied Organometallic Chemistry*, 29, 690-697, 2015.

[41] Oladipo AA. "MIL-53 (Fe)-based photo-sensitive composite for degradation of organochlorinated herbicide and enhanced reduction of Cr(VI)". *Process Safety and Environmental Protection*, 116, 413-423, 2018.

[42] Jiang F, Zheng Z, Xu Z, Zheng S, Guo Z, Chen L. "Aqueous Cr(VI) photoreduction catalyzed by TiO_2 and sulfated TiO_2". *Journal of Hazardous Materials*, 134(1-3), 94-103, 2006.

[43] Chakrabarti S, Chaudhuri B, Bhattacharjee S, Ray AK, Dutta BK. "Photoreduction of hexavalent chromium in aqueous solution in the presence of zincoxide as semiconductor catalyst". *Chemical Engineering Journal,* 153(1-3), 86-93, 2009.

[44] Kabra K, Chaudhary R. "Treatment of hazardous organic and inorganic compounds through aqueous-phase photocatalysis". *Industrial & Engineering Chemistry Research*, 43(24), 7683-7696, 2004.

[45] Cappelletti G, Bianchi CL, Ardizzone S. "Nano-titania assisted photoreduction of Cr(VI): The role of the different TiO_2 polymorphs". *Applied Catalysis B: Environmental*, 78(3-4), 193-201, 2008.

[46] Zhou M, Yu J, Cheng B. "Effects of Fe-doping on the photocatalytic activity of mesoporous TiO_2 powders prepared by an ultrasonic method". *Journal of Hazardous Materials*, 137(3), 1838-1847, 2006.

[47] Ku Y, Jung IL. "Photocatalytic reduction of Cr(VI) in aqueous solutions by UV irradiation with the presence of titanium dioxide". *Water Research*, 35, 135-142, 2001.

[48] Hoffmann MR, Martin ST, Choi W, Bahnemann D. "Environmental applications of semiconductor photocatalysis". *Chemical Reviews*, 95, 69-96, 1995.

[49] Grela MA, Loeb B, Restrepo GM, Lagorio MG. *Román ES. Los Mecanismos De Destrucción.* Ed. Miguel Blesa, Capítulo 5 en: Eliminación de Contaminantes por Fotocatálisis Heterogénea, 8th ed. 125-162, La Plata, Buenos Aires, Argentina, 2004.

[50] Grela MA, Colussi AJ. "Kinetics of stochastic charge transfer and recombination events in semiconductor colloids, relevance to photocatalysis efficiency". *The Journal of Physical Chemistry*, 100, 18214-18221, 1996.

[51] Kamat PV. "Manipulation of charge transfer across semiconductor interface. A criterion that cannot be ignored in photocatalyst design". *The Journal of Physical Chemistry Letters*, 3, 663-671, 2012.

[52] Martin ST, Herrmann H, Hoffmann MR. "Time-resolved microwave conductivity. Part 2.-Quantum-sized TiO_2, and the effect of adsorbates and light intensity on charge-carrier dynamics". *Journal of the Chemical Society, Faraday Transactions*, 90, 3323-3330, 1994.

[53] Meichtry JM, Brusa M, Mailhot G, Grela MA, Litter MI. "Heterogeneous photocatalysis of Cr(VI) in the presence of citric acid over TiO_2 particles: relevance of Cr(V) citrate complexes''. *Applied Catalysis B*, 71, 101-107, 2007.

[54] Meichtry JM, Colbeau-Justin C, Custo G, Litter MI. "TiO_2-photocatalytic transformation of Cr(VI) in the presence of EDTA: comparison of different commercial photocatalysts and studies by time resolved microwave conductivity''. *Applied Catalysis B*, 144, 189-195, 2014.

[55] Montesinos VN, Salou C, Meichtry JM, Colbeau-Justin C. "Litter MI Role of Cr(III) deposition during the photocatalytic transformation of hexavalent chromium and citric acid over commercial TiO_2 samples". *Photochemical & Photobiological Sciences*, 15, 228-234, 2016.

[56] Ananpattarachai J, Kumket P, Tung TV, Kajitvichyanukul P. "Chromium (VI) removal using nano-TiO_2/chitosan film in photocatalytic System". *International Journal of Environment and Waste Management*, 16, 55-70, 2015.

[57] Wang N, Xu Y, Zhu L, Shen X, Tang H. "Reconsideration to the deactivation of TiO_2 catalyst during simultaneous photocatalytic reduction of Cr(VI) and oxidation of salicylic acid". *Journal of Photochemistry*, 201(2-3), 121-127, 2009.

[58] Meichtry JM, Dillert R, Bahnemann D, Litter MI. "Application of the stopped flow technique to the TiO_2-heterogeneous photocatalysis of hexavalent chromium in aqueous suspensions: comparison with O_2 and H_2O_2 as electron acceptors". *Langmuir*, 31, 6229-6236, 2015.